Mahinda *et al.*
*Journal of Engineering and Applied Science* (2023) 70:85
https://doi.org/10.1186/s44147-023-00256-y

Journal of Engineering and Applied Science

RESEARCH Open Access

# Optimal control of a grid-connected photovoltaic agricultural water pumping system

Mercy W. Mahinda[1,2*], Evan M. Wanjiru[1,2†] and Jackson G. Njiri[1,2†]

†Evan M. Wanjiru and Jackson G. Njiri contributed equally to this work.

*Correspondence: eng.wmahinda@gmail.com

[1] Department of Mechatronic Engineering, PAUSTI, Nairobi, Kenya
[2] Department of Mechatronic Engineering, JKUAT, Nairobi, Kenya

## Abstract

Optimization of water pumping systems has been studied using various techniques which include classical, mathematical, and heuristics. Few studies have explored use of optimal controllers in agricultural water pumping applications. Some studies also ignore the interconnection between the water demand and energy used. Introduction of renewable energy sources such as photovoltaic (PV) necessitates different geographical studies as the intensity of the renewable energy varies widely with location. In this paper, an optimal controller for a batteryless grid-connected photovoltaic system to power water supply system for irrigation purposes was developed. The aim was to minimize the operational cost of grid energy by maximizing utilization of photovoltaic power and minimizing the utilization of grid power. A case study was done at a farm in Kajiado (−1.6033257° latitude and 36.7863352° longitude). The farm photovoltaic, grid power, water pumps (underground and booster pump), and storage tanks were modelled into a binary linear programming optimization problem and solved using intlinprog solver on MATLAB. Energy demand data was collected using a three-phase power logger, while water demand data was collected using onsite water meter and stopwatch timer. Photovoltaic power produced was estimated using Photovoltaic Geographical Information System (PVGIS). Simulation results obtained show that the use of an optimal controller results in reduced cost of energy by 44.4%. Better utilization of renewable photovoltaic energy by 24% was observed, and 3.6% more water was pumped.

**Keywords:** Renewable energy, Photovoltaics, Energy cost optimization, Optimal control

## Introduction

Sustainable development goals on zero hunger, good health and wellbeing, clean water and sanitation, and affordable and clean energy are closely linked giving rise to the food-water-energy nexus. In 2017, a joint WHO/UNICEF monitoring program showed that 844 million people lack access to basic drinking water services [1]. Studies have shown that most photovoltaic water pumping systems are oversized. Photovoltaic plants are sized to take care of months that have the worst solar irradiation. This means there are periods when power produced is more than the demand. In the case of agricultural use, water demand for irrigation varies widely based on crop type, stage of growth, weather, etc. Photovoltaic water pumping system for horticultural crop irrigation showed that the

systems are oversized as water demand is not constant throughout the crop productive cycle [2]. A water pumping system for domestic consumption was found to be oversized. The design was based on daily water demand[3]. Oversized renewable energy systems present an opportunity to optimize the use of dumped renewable energy.

Mathematical techniques such as linear programming, mixed integer linear programming, nonlinear programming, and dynamic programming and heuristic techniques such as particle swarm optimization, genetic algorithms, tabu search, and simulated annealing have been used for optimization of water supply systems [4]. Particle swarm optimization is used to solve a pump scheduling problem for flood control with an objective to minimize operational cost. Its results are compared to those based on an expert's experience. Numerical results showed the system can maintain water levels at safe ranges preventing flooding [5]. Use of genetic algorithms to develop an optimized water pumping schedule for a water supply network resulted in 15% average energy efficiency [6]. Use of a binary dragonfly algorithm resulted in reduced energy cost of 29.42% [7]. Use of reduced dynamic programming algorithm in comparison to dynamic programming for optimal operation scheduling of a pumping station results in less computation time [8]. Model predictive control is compared with a particle swarm optimization to meet demands and reduce fluctuations in pumping stations so as to prevent damage and depreciation of the system. Particle swarm optimization was not able to reduce the fluctuations, while the model predictive controller achieved this and went further to minimize the total pumped water resulting in reduced cost of water [9]. Linear optimization is used to solve the residential water pumping schedule using time of use. Comparison between manual operation and the optimal solution results in same energy use but a reduced cost of energy by 18.29% [10]. Water pumping activities that include renewable energy are optimized using mixed integer nonlinear programming; the model results in reduced energy costs by 21.56% [11]. Control optimization based on off-peak and peak periods with inclusion of additional time slots for trigger levels resulted in reduced number of pump switches [12]. A scheduling algorithm based on linear programming and heuristics with demand response consideration showed reduced power demand by 11.2% during the demand response period. The system was able to meet all operational constraints [13]. Introduction of a renewable energy source and use of optimal controllers resulted in a reduced grid energy cost of 33.8% [14]. Use of linear programming to optimize cost of a grid-connected photovoltaic with ground pumped hydro storage system showed a reduced cost of energy from US $6.24 using grid-only supply to US $3.47 with grid-connected pumped hydro storage with minimum initial volume and $0.95 at maximum initial volume of water stored [15]. A photovoltaic underground pumped-hydro storage system with an optimal energy management algorithm based on linear programming resulted in a 32.4% saving in comparison to the baseline [16]. Two control systems are explored for a water pumping system in a water treatment plan. In timer switching that is manually operated and optimal controller based on time of use tariff, the optimal controller results in a cost reduction of 1994 ZAR [17]. Linear programming shows 95% savings in winter in comparison to the baseline [18]. Grid-only supply is compared to grid-interactive pumped hydro storage with an optimal controller; the results are a reduced cost of energy consumed by 68.44% [19]. Optimal control model for a hybrid system results in potential energy savings of 71.3% [20]. A mixed integer

programming model was studied for application in the supply of water for a city. Cost savings were estimated to be about US $255,503.48 [21].

From the studies done, most of the water pumping optimization problems were based on dynamic pricing of electricity through time of use tariffs or demand response programs with incentives. Where standalone hybrid energy systems incorporating renewable energy were used, battery storage was provided. Batteryless hybrid renewable energy systems were grid connected with an option of selling surplus renewable energy back to the grid through net metering. In the review, no studies were found that explored batteryless grid-connected systems with RE based on a fixed grid price with no net metering available. Also, application of optimal controllers in small-scale agricultural water pumping applications are few. Studies including use of photovoltaic systems within the geographical zone of the case study are not available.

Developments in adoption of modern agricultural technology is still limited to developed countries. This is mostly due to lack of resources in the developing countries, and therefore, traditional farming practices based on farmers intuition and experience are still used [22]. Mechanical power, automation, control, and robotics in large-scale agricultural fields are generally associated with developed countries. This results in low productivity and high cost of production. Even with a lot of advancements in agricultural technology, adoption remains low in Africa and Asia [23]. When consideration for adoption of innovative agricultural practices is done, concentration is mostly on the large-scale application as they look at cost-effectiveness [24]. Agriculture is an important pillar in economic development of developing countries that are characterized by mostly small-scale farmers. In Kenya, the area of the case study, cost of grid power is higher than the cost of adopting photovoltaic, and therefore, more people are finding grid-connected systems cost-effective as a way of saving on cost of energy. However, due to the fact the cost of batteries is quite prohibitive, most of these systems have no battery backup. Net metering is not available in the country, and therefore, that means any surplus renewable energy is dumped.

This paper introduces a novel optimal controller for a batteryless grid-connected photovoltaic ground water pumping system applicable in small-scale farms in developing nations. It will find its use in agricultural power supply systems integrating renewable photovoltaic energy without a battery backup and no net metering. The drop in cost of photovoltaic systems coupled with diminishing sources of water has led to a rise in grid-connected photovoltaic systems for ground water pumping in developing nations. However, to minimize the investment costs, such systems are manually controlled, which is not optimal. The proposed controller seeks to maximize on the use of solar energy to power the equipment while meeting the water demand in the farm and minimizing water wastage through spillage. The controller also minimizes the frequent switching of the ground water pump, thereby increasing the pumps and systems life. The main contributions of this paper are as follows:

- The development of an optimal controller that wholistically manages all available resources, i.e., sources of power (PV and grid) and the loads (water pumps) to meet demand for water at minimum cost
- A controller that curtails dumped renewable energy

- A solution that can be easily adopted without necessarily making an investment in the existing farm infrastructure

The paper is structured as follows: section Methods presents the methods, section Optimization model formulation the optimization model formulation, section Results and discussion results and discussion, and with section Conclusions being the conclusions.

## Methods

The research aim was to develop an optimal controller that optimizes energy cost associated with agricultural water pumping applications. Quantitative primary data was collected at a farm in Kajiado. The farm has a photovoltaic plant capacity of 10.56 kW and is connected to grid power. Water is obtained from a 270-m deep borehole through a 7.5-kW submersible pump. There is also a 1.25-kW booster pump on the farm. The farm is set up as two farms each with its own water storage tanks. The inputs to the optimal controller were the photovoltaic power estimates and the water demand. Photovoltaic power estimates were done using Photovoltaic Geographical Information System [25] by inputing the farm location and the month of the study, February. PVGIS was chosen as it has been studied and found suitable for simulating PV yield in East Africa [26]. This estimate was then subjected to losses brought about by the various system components as shown in Eq. (1).

$$P_{pv}(t) = (PVGIS_{estimate}(t) \times A_{pv} \times \eta_{PV} \times \eta_{inv})/1000, \tag{1}$$

where $P_{pv}$ denotes the power from the photovoltaic plant in kW, $PVGIS_{estimate}$ denotes the output from PVGIS in watts/m$^2$, $A_{pv}$ denotes the area of the photovoltaic plant in m$^2$, $\eta_{PV}$ represents the solar panel efficiency, and $\eta_{inv}$ denotes the inverter efficiency.

Water demand data was recorded using the onsite water meter and also a stopwatch timer to determine rate of water utilization. This was done for a 24-h period, a day. To determine energy demand, the power ratings of the pumps were used, and the same was validated using a three-phase energy logger. Periods of pump operation were also recorded when the system was being manually controlled. The cost of energy to power the underground pump in USD is given by Eq. (2).

$$CE_{ug} = P_{ug} \times t \times C, \tag{2}$$

where $CE_{ug}$ denotes cost of energy to power the underground pump in USD, $P_{ug}$ is the underground pump power rating in kW, $t$ is the time the underground pump was running using power supplied by the grid in hours, and $C$ is the cost of energy per kWh as charged by the grid supplier in USD.

The cost of energy to power the booster pump in USD is given by Eq. (3).

$$CE_b = P_b \times t \times C, \tag{3}$$

where $CE_b$ denotes cost of energy to power the booster pump, $P_b$ is the booster pump power rating in kW, $t$ is the time the booster pump was running using power supplied by the grid in hours, and $C$ is the cost of energy per kWh as charged by the grid supplier.

Total cost of energy used from the grid supplier is the summation of $CE_{ug}$ and $CE_b$. This would then form the basis for comparison between manual and optimal control.

**Table 1** Solar panel properties and installation parameters

| Table of solar panel properties and installation | |
|---|---|
| Model | Yingli YL330P-35b |
| Efficiency | 16.46% |
| STC power rating | 330 W |
| Rated voltage | 37.3 V |
| Rated current | 8.85 A |
| Number of panels | 32 |
| Dimensions | Length 2000 mm, width 992 mm, depth 40 mm |
| Area per panel | 1.984 $m^2$ |
| Solar farm area | 63.488 $m^2$ |
| Tilt | 10 ° |
| Azimuth | 180 ° |

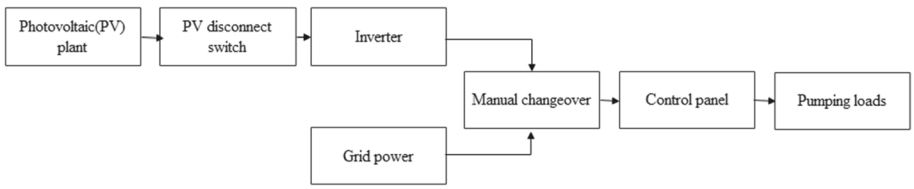


**Fig. 1** Power supply system for water pumping

Diagrams were developed using Wondershare EdrawMax software. The optimal control algorithm was developed using MATLAB and solved using intlinprog.

## Optimization model formulation

### Case study

A case study was done at a farm located in Kajiado, Kenya (−1.6033257° latitude and 36.7863352° longitude). The farm has an already installed photovoltaic (PV) plant capacity of 10.56 kW comprising of 32 solar panels rated at 330 Wp. Properties of the solar panels and installation parameters are as in Table 1.

The solar panels are then connected to the Dayliff Sunverter 2, model SV2/11T through the PV disconnect switch as shown in Fig. 1.

The inverter efficiency is 99%; this can be found in the manual [27].

Output from the inverter meets with the grid power supply at a manual changeover switch. The output from the manual changeover switch goes through the control panel to the underground pump as shown in Fig. 1 above.

There is a 270-m deep borehole that supplies water for drip irrigation, watering 100 goats and also for domestic use. Some of the locals also purchase the water, and it is not unusual to see school-going children passing by during the evening just to quench their thirst. Drinking water is usually obtained from rainwater collected in a 5000-l tank, and when the tank is emptied, the deficit is obtained from the borehole. Water for irrigation is stored in elevated tanks that amount to 43,000 l. The farm is divided into two: farm 1 with an installed water storage capacity of 23,000 l (tank 1 is 10,000 l, tank 2 is 8000

l, and tank 3 is 5000 l) and farm 2 with an installed water storage capacity of 20,000 l (tank 4 is 10,000 l, and tank 5 is 10,000 l) with the arrangement schematically depicted in Fig. 2.

There are two irrigation cycles in a day: in the morning and in the evening. The ground water pump is run by a 3-phase 4GG-4GX 4″ submersible motor rated at 7.5 kW that can supply 150 L/min. Farm 2 is served by a booster pump, Pedrollo pump rated at 1.25 kW that supplies 90 L/min. The energy demand data is collected using three-phase energy logger, and photovoltaic power is estimated using PVGIS tool [25] and taking into consideration the efficiency of the solar panels and the inverter, while water demand is measured using the onsite water meter and stopwatch timer.

### Manual control

Hourly energy and water demand data was collected for a day in the month of February resulting in 24 sampling periods (N). February is the hottest month of the year, and therefore, demand for water is highest during this month with the highest average temperature, 27.43 ° recorded at noon. Farm 1 had two irrigation cycles from 07:00 to 10:00 h in the morning and from 16:00 to 20:00 h in the evening. Farm 2 had one irrigation cycle in the evening from 16:00 to 21:00 h. Total water demand for the day was 55,000 l with farm 1 requiring 35,000 l and farm 2 requiring 20,000 l as shown in Fig. 3.

Photovoltaic power estimate using PVGIS for the month of february is as in Fig. 4.

Using manual control of the power supply system, water was pumped using grid energy from 06:00 to 09:00 h bringing the total time the underground water pump was on grid to 3 h. Thereafter, energy used was supplied by the photovoltaic system for 3 h and 7 min until the tanks were full (see Fig. 5). This schedule was based on the farm managers intuition on how to operate the system.

The booster pump is only connected to grid power; therefore, all energy used for the 3 h 43 min it was running from 13:00 to 16:43 h was supplied by grid. At the end of the day, the elevated water storage tanks were left empty. Applying a cost of US $0.16 per kWh for small commercial as charged by the grid supplier, the cost of

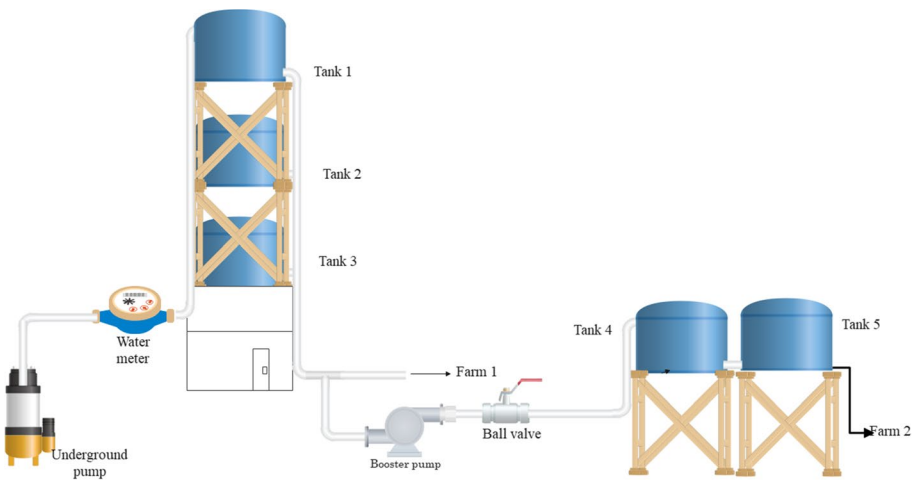


**Fig. 2** Water supply system for both farm 1 and farm 2

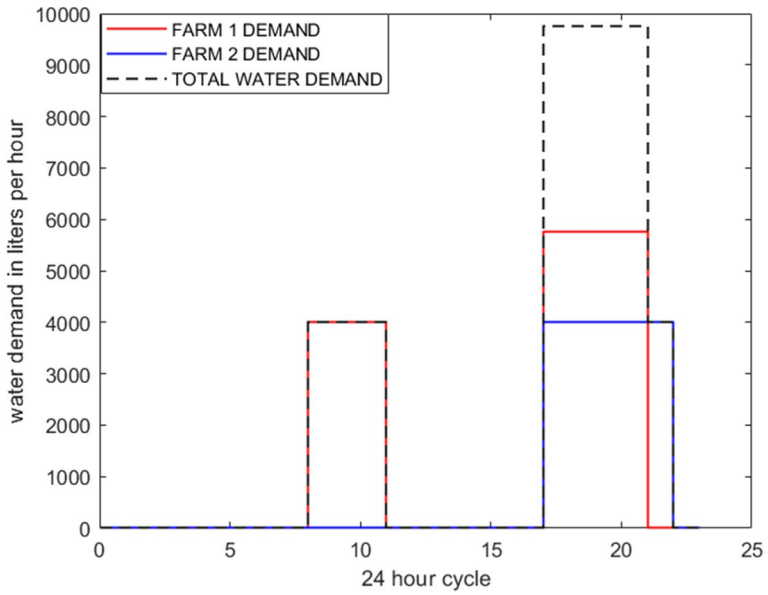


**Fig. 3** Water demand for farm 1 and farm 2

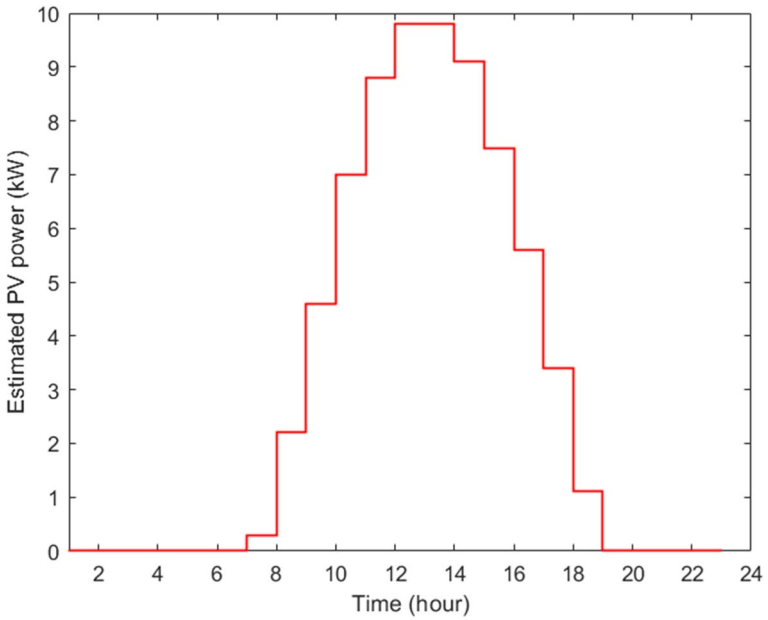


**Fig. 4** Photovoltaic power estimate using PVGIS

running the underground pump on grid power for 3 h comes to US $3.6 per day, and that of running the booster pump for 3 h 43 min comes to US $0.74. Total daily energy utilized by the underground pump was 45.88 kWh and 4.65 kWh by the booster pump. Total energy cost of running pumping operations on the farm for the 24 h period came to US $4.34.

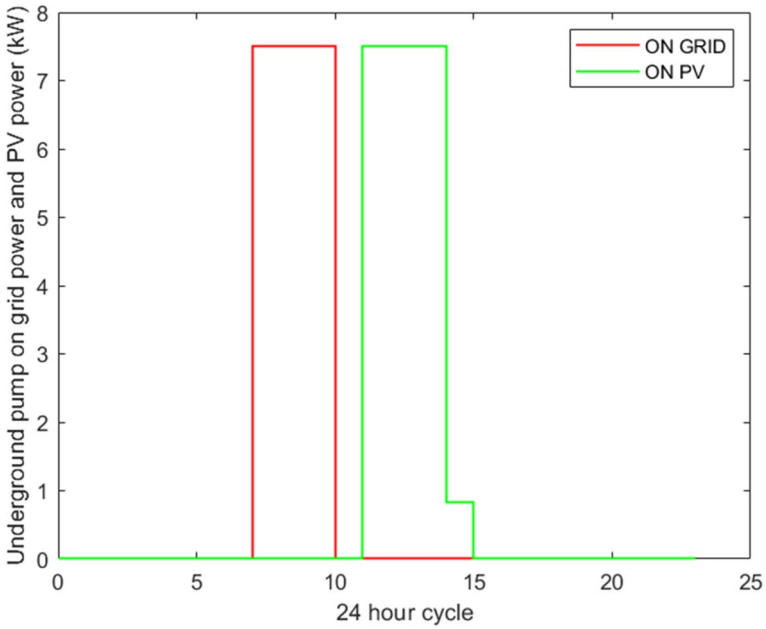


**Fig. 5** Grid and photovoltaic power utilization under manual control

### System components

The entire system consists of grid power, photovoltaic power, isolator switch, inverter, manual changeover switch, control panel, undergound pump, booster pump, water meter, and elevated water storage tanks.

#### *Grid*

Grid power is supplied by the utility provider and charged per kWh consumed. Supply from the grid can be a minimum of zero, and the maximum value is the maximum load being provided for as in Eq. (5).

$$0 \leq P_{grid} u_g(t) \leq P_{maxLoad}, \tag{4}$$

where $P_{grid}$ denotes grid power supply in kW, $u_g(t)$ represents the status of the grid power supply (ON or OFF), and $P_{maxLoad}$ denotes the maximum load in kW.

#### *Solar PV power*

Photovoltaic (PV) system consists of modules/panels connected in series or parallel. They take light supplied by the sun and convert it into electrical power. Solar power obtained from the photovoltaic panels is dependent on solar irradiance and the temperature of the panels [28]. This is shown in Eq. (5).

$$P_{PV}(t) = \left( \frac{(P_{STC} + \alpha_{PV}(T_{cell}(t) - T_{STC}))G(t)}{1000} \right), \tag{5}$$

where $P_{PV}(t)$ denotes photovoltaic power in kW/m$^2$, $P_{STC}$ represents the power in standard test conditions in watts, $\alpha_{PV}$ represents the temperature coefficient of power in watts/ °C, $T_{cell}(t)$ denotes the surface PV cell temperature in °C, $T_{STC}$ represents the

standard test conditions temperature in °C, and $G(t)$ denotes the solar irradiance at a given time in W/m$^2$

An isolator switch is used to de-energize the photovoltaic system during maintenance.

Inverter converts the direct current (DC) supplied by the photovoltaic plant into alternating current (AC) for used by the AC loads [29]. Power supplied by the inverter is presented as Eq. (6).

$$P_{inv}(t) = P_{pv}(t)\eta_{inv}, \tag{6}$$

where $P_{pv}$(t) denotes the power from the photovoltaic panels at a given time, $\eta_{inv}$ denotes inverter efficiency, and $P_{inv}$(t) represents the output power from the inverter at a given time.

#### *Water pumps*

Underground pump delivers water from the borehole to the raised tanks. There are two main types of pumps: positive displacement pumps that are suited for lower flow rates and medium-to-high-pumping heads and centrifugal pumps suited for high flow rates and lower pumping heads. Normally, a submersible pump is used for boreholes [30], and a fixed speed submersible pump was considered in this study.

The booster pump is used to increase the water pressure and hence water flow rates for water being delivered at longer distances. The booster pump was used to boost water pressure from farm 1 supply to farm 2 which is far from the borehole supply. In this study, a fixed speed booster pump was considered. Given that both pumps were fixed speed pumps, then their status (ON or OFF) was mathematically modelled as given in Eqs. (7) and (8).

$$u_{ug}(t) \in \{0, 1\} \tag{7}$$

$$u_b(t) \in \{0, 1\} \tag{8}$$

where $u_{ug}$(t) and $u_b$(t) are the status of the underground and booster pumps respectively.

### Optimization model

Figure 6 shows the block diagram illustrating the general flow of optimization. Water demand and PV power estimates are inputs to the optimal controller which then outputs ON/OFF signals to the power supply that will be used between the grid and the photovoltaic plant. And ON/OFF signals to the pumping loads to supply water to the storage tanks which is then used to meet demand.

#### *Power balance*

The power balance equation in continuous time domain is represented by Eq. (9).

$$P_{ug}u_{ug}(t) - P_{grid}u_g(t) + P_b u_b(t) - P_{pv}(t)u_{pv}(t) \leq 0 \tag{9}$$

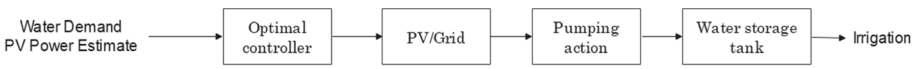


**Fig. 6** Block diagram optimization flow

Here, $P_{ug}$ denotes the underground pump power rating in kW, $P_{grid}$ represents grid power in kW, $P_b$ denotes the booster pump power rating in kW, $P_{pv}(t)$ represents power available from the photovoltaic system in kW, $u_{ug}(t)$ is the status of the underground pump (ON or OFF), $u_g(t)$ is the status of the grid on the manual changeover switch (ON or OFF), $u_b(t)$ is the status of the booster pump (ON or OFF), and $u_{pv}$ is the status of the photovoltaic system on the manual changeover switch (ON or OFF). The power demand by the loads (underground and booster pumps) should always be less or equal to the power supplied in the grid or the photovoltaic system. This ensures demand is met all the time.

#### *Dynamics of water flow*

Dynamics of water volume within the storage tanks in continuous time domain is given by the following:

$$\dot{V} = (InF)u(t) - OtF(t), \tag{10}$$

where $\dot{V}$ represents the rate of change of volume of water in the storage tank, $InF$ represents pump flow rate in liters per hour, $OtF$ is the water flowing out of the tank due to demand in liters per hour, and $u(t)$ is the status of the pump (ON or OFF). In discrete-time domain, Eq. (10) is expressed as follows:

$$V(j+1) = V(j) + t_s(InF)u(j) - t_sOtF(j), \tag{11}$$

After recurrent manipulation, then the dynamic of water flow in any of the tanks can be modelled as in Eq. (12).

$$V(j) = V(0) + \sum_{i=1}^{j} (t_s(InF)u(i) - t_sOtF(i)), \tag{12}$$

where $V(0)$ denotes the initial water volume in tank in liters and $t_s$ represents the time sample in hours.

#### *Objective function*

Objective function is to minimize the operational cost of grid energy and the maintenance cost. The general optimization problem will follow the Eqs. (13) to (15) [31].

$$minJ(x), \tag{13}$$

Subject to

$$g(x) = 0, \tag{14}$$

$$h(x) \leq 0. \tag{15}$$

where $x$ denotes the optimization variable, $J(x)$ denotes the objective function, $g(x)$ denotes the equality constraint, and $h(x)$ denotes inequality constraint.

In the process of optimizing operational cost of energy, the underground pump might switch ON/OFF too many times, which is undesirable as it will result in increased cost of maintenance due to wear and tear. Using the Pretoria method, an auxiliary variable $s(j)$ is

introduced that takes a value of 1 whenever a start-up happens [32]. The objective function is given by Eq. (16).

$$J = \sum_{j=1}^{N} \left( w_1 P_{ug} t_s C u_{ug}(j) + w_2 P_b t_s C u_b(j) + w_3 s(j) \right), \tag{16}$$

where $N$ denotes the number of time samples, $w_1$ denotes the weighting factor associated with energy cost of the underground pump, $t_s$ denotes the time sample in hours, $C$ represents the cost of grid power in USD, $u_{ug}(j)$ denotes the decision variable associated with the underground pump state (ON or OFF), $w_2$ denotes the weighting factor associated with energy cost of the booster pump, $u_b(j)$ represents the decision variable associated with the booster pump state (ON or OFF), $w_3$ denotes the weighting factor associated with pump maintenance cost, and $s(j)$ is the auxiliary variable. Here,

$$w_1 + w_2 + w_3 = 1 \tag{17}$$

#### *Constraints/variables*

At any given instance, the power supplied by the grid and the photovoltaic plant should always be greater or equal to the load. This is to ensure that energy demand needs are met at all times.

$$P_{grid}(j) u_g(j) + P_{pv}(j) u_{pv}(j) \geq P_{ug} u_{ug}(j) + P_b u_b(j), \tag{18}$$

Representating Eq. (18) in canonical form shown in Eq. (15).

$$P_{ug} u_{ug}(j) - P_{grid}(j) u_g(j) + P_b u_b(j) - P_{pv}(j) u_{pv}(j) \leq 0 \tag{19}$$

Furthermore, Eq. (19) can be written in matrix form yielding A1 and b1:

$$\begin{bmatrix} P_{ug}(1) \ldots P_{ug}(N) & -P_{grid}(1) \cdots -P_{grid}(N) & P_b(1) \ldots P_b(N) & -P_{pv}(1) \cdots -P_{pv}(N) & 0(1) \ldots 0(N) \end{bmatrix} \begin{bmatrix} u_{ug}(1) \\ \vdots \\ u_{ug}(N) \\ u_g(1) \\ \vdots \\ u_g(N) \\ u_b(1) \\ \vdots \\ u_b(N) \\ u_{pv}(1) \\ \vdots \\ u_{pv}(N) \\ s(1) \\ \vdots \\ s(N) \end{bmatrix} \leq 0, \tag{20}$$

The power supplied can either come from the photovoltaic plant or the grid due to the manual changeover switch. This is represented by Eq. (21).

$$U_g(j) + U_{pv}(j) \leq 1, \tag{21}$$

Equation (21) in matrix form yields A2 and b2:

$$\begin{bmatrix} 0(1)\ldots 0(N) & 1(1)\ldots 1(N) & 0(1)\ldots 0(N) & 1(1)\ldots 1(N) & 0(1)\ldots 0(N) \end{bmatrix} \begin{bmatrix} u_{ug}(1) \\ \vdots \\ u_{ug}(N) \\ u_g(1) \\ \vdots \\ u_g(N) \\ u_b(1) \\ \vdots \\ u_b(N) \\ u_{pv}(1) \\ \vdots \\ u_{pv}(N) \\ s(1) \\ \vdots \\ s(N) \end{bmatrix} \leq 1 \tag{22}$$

Constraints and variables associated with the water storage system in farm 1 are given by Eq. (23). Farm 1 has an installed water storage capacity of 23,000 l. This is the maximum possible amount of water that can be stored without spillage. There is also a minimum set water volume level that is at the discretion of the designer to ensure demand is met at all times.

$$V_{min} \leq V(0) + \sum_{i=1}^{j} \left( InF_1 t_s u_{ug}(i) - OtF_{12} t_s u_b(i) - OtF_1(i) t_s \right) \leq V_{max} \tag{23}$$

Here, $V_{min}$ denotes the allowable minimum water stored within the storage tanks in liters, $V(0)$ represents initial water volume in the storage tanks in liters, $j$ denotes the number of time samples, $InF_1$ represents water flowing into farm 1 storage tanks as supplied by the underground pump in liters per hour, $t_s$ denotes the time sample in hours, $OtF_{12}$ represents water flowing out of farm 1 storage tanks into farm 2 storage tanks through the booster pump in liters per hour, $OtF_1(i)$ represents water flowing out of farm 1 storage tanks to meet water demand requirements for farm 1 in liters per hour, and $V_{max}$ denotes the maximum water volume that can be stored by the tanks in liters.

The linear inequality constraint (23) can be represented in the canonical form shown in Eq. (15) as Eq. (24).

$$-\sum_{i=1}^{j} \left( InF_1 t_s u_{ug}(i) - OtF_{12} t_s u_b(i) \right) \leq -V_{min} + V(0) - \sum_{i=1}^{j} OtF_1(i) t_s, \tag{24}$$

Equation (24) in matrix form yields A3 and b3.

$$A3 = \begin{bmatrix} -InF_1t_s & 0 & 0 & \dots & 0 & 0 & \dots & 0 & OtF_{12}t_s & 0 & 0 & \dots & 0 & 0 \dots & 0 & 0 \dots & 0 \\ -InF_1t_s & -InF_1t_s & 0 & \dots & 0 & 0 & \dots & 0 & OtF_{12}t_s & OtF_{12}t_s & 0 & \dots & 0 & 0 \dots & 0 & 0 \dots & 0 \\ \vdots & \vdots & \ddots & \vdots & \vdots & \vdots & \ddots & \vdots & \vdots & \vdots & \ddots & \ddots & \vdots & \vdots & \vdots & \vdots & \vdots \\ -InF_1t_s & -InF_1t_s & -InF_1t_s & \dots & -InF_1t_s & 0 & \dots & 0 & OtF_{12}t_s & OtF_{12}t_s & OtF_{12}t_s & \dots & OtF_{12}t_s & 0 \dots & 0 & 0 \dots & 0 \end{bmatrix} \tag{25}$$

$$b3 = \begin{bmatrix} -V_{min} + V(0) - OtF_1(1)t_s \\ -V_{min} + V(0) - (OtF_1(1)t_s + OtF_1(2)t_s) \\ \vdots \\ -V_{min} + V(0) - (OtF_1(1)t_s + OtF_1(2)t_s + \dots OtF_1(N)t_s) \end{bmatrix} \tag{26}$$

The linear inequality constraint (23) can be represented in the canonical form shown in Eq. (15) as Eq. (27).

$$\sum_{i=1}^{j} (InF_1t_su_{ug}(i) - OtF_{12}t_su_b(i)) \leq V_{max} - V(0) + \sum_{i=1}^{j} OtF_1(i)t_s, \tag{27}$$

Equation (27) in matrix form yields A4 and b4.

$$A4 = \begin{bmatrix} InF_1t_s & 0 & 0 & \dots & 0 & 0 & \dots & 0 & -OtF_{12}t_s & 0 & 0 & \dots & 0 & 0 \dots & 0 & 0 \dots & 0 \\ InF_1t_s & InF_1t_s & 0 & \dots & 0 & 0 & \dots & 0 & -OtF_{12}t_s & -OtF_{12}t_s & 0 & \dots & 0 & 0 \dots & 0 & 0 \dots & 0 \\ \vdots & \vdots & \ddots & \vdots & \vdots & \vdots & \ddots & \vdots & \vdots & \vdots & \ddots & \ddots & \vdots & \vdots & \vdots & \vdots & \vdots \\ InF_1t_s & InF_1t_s & InF_1t_s & \dots & InF_1t_s & 0 & \dots & 0 & -OtF_{12}t_s & -OtF_{12}t_s & -OtF_{12}t_s & \dots & -OtF_{12}t_s & 0 \dots & 0 & 0 \dots & 0 \end{bmatrix} \tag{28}$$

$$A4 = -A3 \tag{29}$$

$$b4 = \begin{bmatrix} V_{max} - V(0) + OtF_1(1)t_s \\ V_{max} - V(0) + (OtF_1(1)t_s + OtF_1(2)t_s) \\ \vdots \\ V_{max} - V(0) + (OtF_1(1)t_s + OtF_1(2)t_s + \dots OtF_1(N)t_s) \end{bmatrix} \tag{30}$$

Constraints and variables associated with the water storage system in farm 2 are given by Eq. (31). Farm 2 has an installed water storage capacity of 20,000 l. This is the maximum possible amount of water that can be stored without spillage. There is also a minimum set water volume level that is at the discretion of the designer to ensure demand is met at all times.

$$V_{min} \leq V(0) + \sum_{i=1}^{j} (InF_2t_su_b(i) - OtF_2(i)t_s) \leq V_{max} \tag{31}$$

Note: $InF_2$ is equal to $OtF_{12}$. Here, $InF_2$ represents the water flowing into the storage tanks as supplied by the booster pump in liters per hour, and $OtF_2$ represents water flowing out of farm 2 storage tanks to meet water demand requirements for farm 2 in liters per hour. The linear inequality constraint (31) can be represented in the canonical form shown in Eq. (15) as Eq. (32).

$$-\sum_{i=1}^{j} OtF_{12}t_s u_b(i) \leq -V_{min} + V(0) - \sum_{i=1}^{j} OtF_2(i)t_s, \tag{32}$$

Equation (32) represented in standard matrix form yields A5 and b5.

$$A5 = \begin{bmatrix} 0 & \dots & 0 & 0 & \dots & 0 & -OtF_{12}t_s & 0 & \dots & 0 & 0 & \dots & 0 & 0 & \dots & 0 \\ 0 & \dots & 0 & 0 & \dots & 0 & -OtF_{12}t_s & -OtF_{12}t_s & \dots & 0 & 0 & \dots & 0 & 0 & \dots & 0 \\ \vdots & \ddots & \vdots & \vdots & \ddots & \vdots & \vdots & \vdots & \ddots & \vdots & \vdots & \ddots & \vdots & \vdots & \ddots & \vdots \\ 0 & \dots & 0 & 0 & \dots & 0 & -OtF_{12}t_s & -OtF_{12}t_s & \dots & -OtF_{12}t_s & 0 & \dots & 0 & 0 & \dots & 0 \end{bmatrix} \tag{33}$$

$$b5 = \begin{bmatrix} -V_{min} + V(0) - OtF_2(1)t_s \\ -V_{min} + V(0) - (OtF_2(1)t_s + OtF_2(2)t_s) \\ \vdots \\ -V_{min} + V(0) - (OtF_2(1)t_s + OtF_2(2)t_s + \dots OtF_2(N)t_s) \end{bmatrix} \tag{34}$$

The linear inequality constraint (31) can be represented in the canonical form shown in Eq. (15) as Eq. (35).

$$\sum_{i=1}^{j} (OtF_{12}t_s u_b(i) \leq V_{max} - V(0) + \sum_{i=1}^{j} OtF_2 t_s \tag{35}$$

Equation (35) in matrix form yields A6 and b6.

$$A6 = \begin{bmatrix} 0 & \dots & 0 & 0 & \dots & 0 & OtF_{12}t_s & 0 & \dots & 0 & 0 & \dots & 0 & 0 & \dots & 0 \\ 0 & \dots & 0 & 0 & \dots & 0 & OtF_{12}t_s & OtF_{12}t_s & \dots & 0 & 0 & \dots & 0 & 0 & \dots & 0 \\ \vdots & \ddots & \vdots & \vdots & \ddots & \vdots & \vdots & \vdots & \ddots & \vdots & \vdots & \ddots & \vdots & \vdots & \ddots & \vdots \\ 0 & \dots & 0 & 0 & \dots & 0 & OtF_{12}t_s & OtF_{12}t_s & \dots & OtF_{12}t_s & 0 & \dots & 0 & 0 & \dots & 0 \end{bmatrix} \tag{36}$$

$$A6 = -A5 \tag{37}$$

$$b6 = \begin{bmatrix} V_{max} - V(0) + OtF_2(1)t_s \\ V_{max} - V(0) + (OtF_2(1)t_s + OtF_2(2)t_s) \\ \vdots \\ V_{max} - V(0) + (OtF_2(1)t_s + OtF_2(2)t_s + \dots OtF_2(N)t_s) \end{bmatrix} \tag{38}$$

The auxiliary variable $s(j)$ is constrained as in Eqs. (39) and (40).

$$u_{ug}(1) - s(1) \leq 0, \tag{39}$$

$$u_{ug}(j) - u_{ug}(j-1) - s(j) \leq 0, \tag{40}$$

where,

$$s(j) \in \{0, 1\}. \tag{41}$$

Matrix A7 and vector b7 representing the auxilliary variable are developed as in (42) and (43), respectively.

$$A7 = \begin{bmatrix} 1 & 0 & 0 & \dots & 0 & 0\,0 & \dots & 0\,0 & \dots & 0\,0 & \dots & 0 & -1 & 0 & 0 & \dots & 0 \\ -1 & 1 & 0 & \dots & 0 & 0\,0 & \dots & 0\,0 & \dots & 0\,0 & \dots & 0 & 0 & -1 & 0 & \dots & 0 \\ 0 & -1 & 1 & \dots & 0 & 0\,0 & \dots & 0\,0 & \dots & 0\,0 & \dots & 0 & 0 & 0 & -1 & \dots & 0 \\ \vdots & \vdots & \vdots & \ddots & \vdots & \vdots\,\vdots & \ddots & \vdots\,\vdots & \ddots & \vdots\,\vdots & \ddots & \vdots & \vdots & \vdots & \vdots & \ddots & 0 \\ 0 & 0 & 0 & \dots & -1 & 1\,0 & \dots & 0\,0 & \dots & 0\,0 & \dots & 0 & 0 & 0 & 0 & \dots & -1 \end{bmatrix} \tag{42}$$

$$b7 = \begin{bmatrix} 0(1) \\ \vdots \\ 0(N) \end{bmatrix} \tag{43}$$

All the decision variables $u_{ug}(1)$,..., $u_{ug}(N)$, $u_g(1)$, ...,$u_g(N)$, $u_b(1)$, ...,$u_b(N)$, $u_{pv}(1)$, ...,$u_{pv}(N)$, $s(j)(1)$, and ...,$s(j)(N)$ have a lower and upper bound of 0 and 1. The objective function, matrices [*A1;A2;A3;A4;A5,A6;A7*], and vectors [*b1;b2;b3;b4;b5;b6;b7*] are put into a MATLAB code, and using intlinprog solver, the optimization problem is solved.

## Results and discussion

Table 2 shows the parameters used for the optimization based on the case study and the developed optimization problem.

### Optimal control simulation

The ON/OFF signals to the pump take a value of 1 for ON and a value of 0 for OFF. They are represented by the red-colored steps. The change in water volume in liters within the water storage tanks as pumps come on and off and demand is met is represented by the blue line.

**Table 2** Table of parameters used in the optimal control simulation

| Table of parameters | |
|---|---|
| Time horizon | 1 day (24 h) |
| Sampling interval ($t_s$) | 20 min (1/3 h) |
| N | Number of time samples, 72 |
| $V_{max}$ farm 1 | 23,000 l |
| $V_{min}$ farm 1 | 0 l |
| $V_{max}$ farm 2 | 20,000 l |
| $V_{min}$ farm 2 | 0 l |
| Underground pump power rating | 7.5 kW |
| Booster pump power rating | 1.25 kW |
| Underground pump flow rate | 9000 l/h |
| Booster pump flow rate | 5400 l/h |
| $w_1$ | 0.4 |
| $w_2$ | 0.4 |
| $w_3$ | 0.2 |
| C | Energy cost per kWh for small commercial at US $$0.16 |

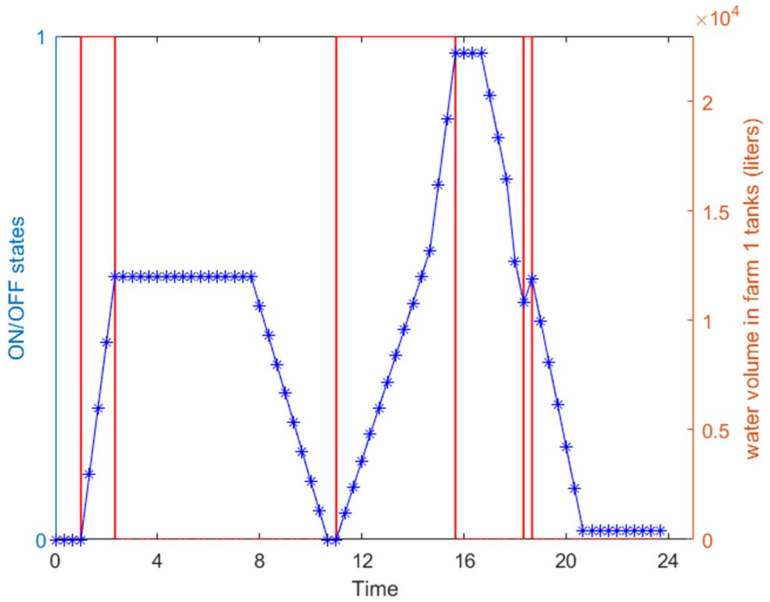


**Fig. 7** Underground pump ON/OFF states and the water storage levels on farm 1

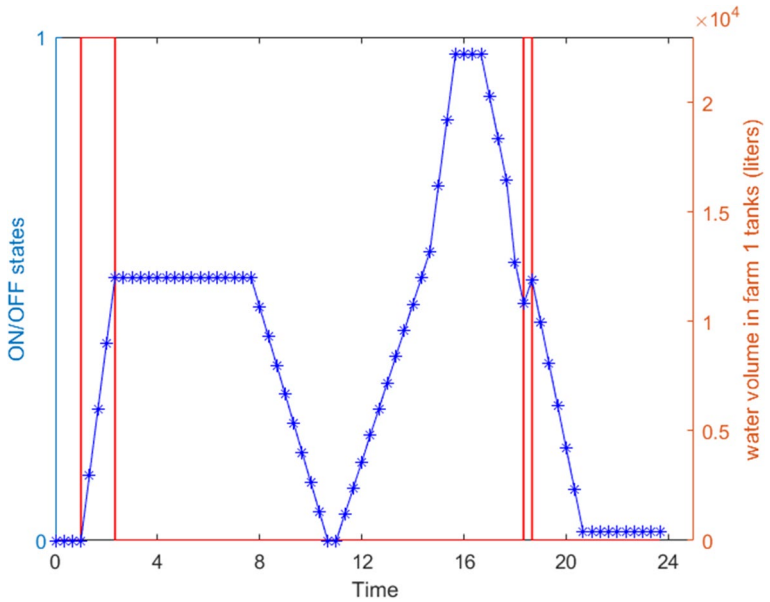


**Fig. 8** Underground pump using grid power and the water storage levels on farm 1

Figure 7 below shows the underground pump running from 01.00 to 02:20 h continuously. During this period, 12,000 l of water is pumped. The underground pump is on grid power as the power produced by the photovoltaic plant is 0 and therefore insufficient to meet the underground pump load. At 07:40 h, demand for farm 1 morning irrigation water needs kicks in taking 12,000 l of water. At the end of the irrigation cycle, the water volume on farm 1 tank storage is left at 0 l. The underground pump is on photovoltaic power from 11.00 h. During this period, photovoltaic

power is supplied, and 8.8 kW is sufficient to meet the power demands of both the underground pump and the booster pump which require 8.75 kW. The underground pump runs continuously for 4 h 40 min up to 15:40 h pumping 42,000 l of water. During this period, the booster pump also runs for 3 h and 40 min taking 19,800 l of water from farm 1 water storage tanks to farm 2 water storage tanks. This leaves 22,200 l in farm 1 water storage tanks. The underground pump goes off at 15:40 h to avoid violating the maximum water storage capacity constraint of 23,000 l, thus avoiding loss of water through spillage. The underground pump comes back on at 18:20 h and runs for 20 min to 18:40 h. During this period, it delivers 3,000 liters of water to meet the demands for irrigation water for both farm 1 and farm 2 requirements. It runs on grid power for the 20 min as the photovoltaic power supplied, 5.6 kw is insufficient to power the underground pump. At the end of the day, 400 l is left in farm 1 water storage tanks. Total energy consumed by the underground pump for the time its running comes to 47.5 kWh. This energy is supplied by both grid and photovoltaic power.

Figure 8 shows the periods the underground pump is on grid power from 01:00 to 02:20 h and from 18:20 to 18:40 h. The energy consumed from grid comes to 12.5 kWh. It therefore costs US $2 to run the underground pump for the day.

Figure 9 shows the booster pump running from 11:00 to 14:40 h; during this period, photovoltaic power produced is sufficient to meet both the pumping loads, i.e., the underground pump and the booster pump. The booster pump supplies 19,800 l of water to farm 2 tank storage for the 3 h 40 min it is on. The booster pump then goes off to avoid violating the maximum water storage capacity constraint of 20,000 l and therefore prevents water loss through spillage. The booster pump comes back on at 17:40 to 18:00 h supplying 1800 l to farm 2 water storage tanks. The booster pump runs on photovoltaic power as the power available from the photovoltaic is sufficient to meet the booster pump load only. In total water supplied by the booster pump,

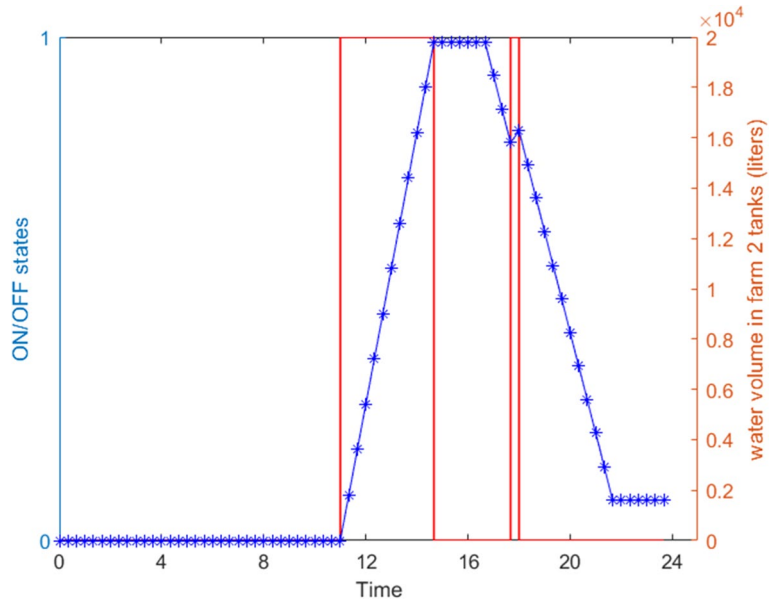


**Fig. 9** Booster pump ON/OFF states and the water storage levels on farm 2

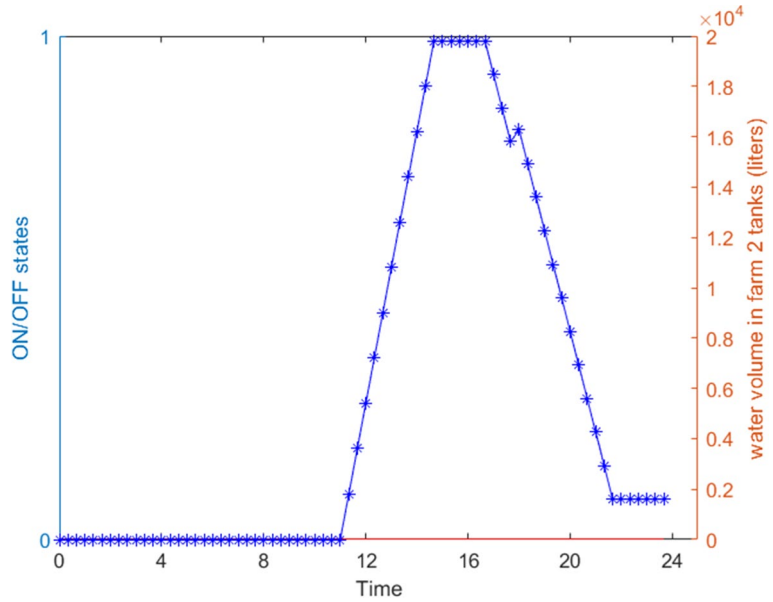


**Fig. 10** Booster pump using grid power and the water storage levels on farm 2

**Table 3** Manual control (baseline) versus optimal control

| **Summary of findings** | | |
|---|---|---|
| | **Manual control** | **Optimal control** |
| Amount of water pumped | 55,000 l | 57,000 l |
| PV energy utilized | 23.4 kWh | 40 kWh |
| PV energy wasted | 45.8 kWh | 29.2 kWh |
| Grid energy utilized | 27.15 kWh | 12.5 kWh |
| Total energy consumed | 50.55 kWh | 52.5 kWh |
| Total energy cost | US $4.34 | US $2 |
| Energy cost per $m^3$ | US $7.89 cents | US $3.5 cents |

21,600 l is sufficient to meet water demands for farm 2 irrigation which amount to 20,000 l. At the end of the day, 1600 l are left in farm 2 water storage tanks. Total energy consumed by the booster pump for the time it is running comes to 5 kWh. This energy is supplied purely by photovoltaic power.

Figure 10 shows the booster pump did not run using grid power. This is because power supplied by the photovoltaic plant was sufficient at all times the booster pump was needed to run so as to meet demand for farm 2.

Assumptions, limitations, and uncertainties of the study:

- The grid power is always available when needed.
- Use of February, the hottest month with the highest water demand as a representation of the whole year.
- Time sample resolution of 20 min as sufficient for the simulation, while smaller resolutions would probably provide a better performance but at a higher computational burden.

- Uncertainties in the unexpected changes in water demand.

Table 3 shows the comparison between the performance of manual (baseline) and optimal control strategies.

Both manual control and optimal control methods pumped sufficient water to meet the demand. The total amount of water pumped using optimal controller is greater than baseline by 3.6%. Under manual control, 66.2% of the photovoltaic energy generated for the day is wasted, while 42.2% photovoltaic energy is wasted under optimal control. Total energy consumed for optimal control is higher than baseline by 3.9%; this can be attributed to more water pumped under optimal control. However, optimal control pumping is cheaper than baseline by 44.4%. This is because optimal control maximized the use of photovoltaic energy leading to better utilization of renewable energy source by 24%.

Given the outcome of the optimal controller in comparison to manual control, it would be prudent for the farm owner to adopt it as an energy cost-saving measure. This can be achieved by replacing the manual changeover switch with automatic control that is based on optimal control. The optimal controller would take the required water demand for the day as an input, the estimated photovoltaic power, and provide optimized start/stop signals to the underground and booster pump. Better utilization of the renewable energy source would be seen giving a better return on investment.

## Conclusions

The results obtained indicate that using optimal controllers can result in energy cost savings. Using simulation results obtained, more energy is consumed using the optimal controller compared to manual control but at a reduced cost of energy by 44.4%. This is achieved by better utilization of the available photovoltaic energy with less RE wasted. At the end of the 24-h cycle, some water is left in storage in both farm 1 and farm 2 providing a buffer which further optimizes next day operational cost. The savings made on the cost of energy are substantial to make a case for adoption of this technology for small-scale farms as it quantifies advantages for adoption to the user. In cases where no funds are available for additional investments, the output of the optimal controller simulation can be adopted as the optimal operation schedule which can then be used by the farm manager as a tool for better day-to-day operation.

This approach will not only be useful for the case presented but also other cases using grid-connected renewable energy systems without battery storage and no option to sell back to the grid. It will mostly find its use with farm managers of small-scale farms and also original equipment manufacturers of solar water pumping solutions as a better control system for managing all the resources available. Further optimization of this approach can be done by directing PV energy wasted to other uses such as desalination of brackish water for domestic consumption and commercial sale.

**Abbreviations**

| | |
|---|---|
| kW | Kilowatt |
| kWh | Kilowatt hour |
| MATLAB | Matrix Laboratory |
| PV | Photovoltaic |

| | |
|---|---|
| PVGIS | Photovoltaic Geographical Information System |
| RE | Renewable energy |
| STC | Standard test conditions |
| USD | United States dollar |
| UNICEF | United Nations International Children's Emergency Fund |
| WHO | World Health Organization |

**Acknowledgements**
This work was supported by the African Union Commission through the Pan African University scholarship.

**Authors' contributions**
MWM conceptualized, worked on the methodology, obtained resources, software, and did the validation, formal analysis, investigation, data collection, project administration, funding request, and writing of the original draft. EMW conceptualized, worked on the methodology, reviewing and editing the original draft, provided resources, and supervision. JGN conceptualized, provided resources, funding acquisition, reviewed and edited the original draft, and provided supervision. All authors read and approved the final manuscript.

**Funding**
This research was made possible through Pan African University scholarship program.

**Availability of data and materials**
Datasets used during the current study are available from the corresponding author on reasonable request.

## Declarations

**Competing interests**
The authors declare that they have no competing interests.

Received: 6 April 2023 Accepted: 12 July 2023
Published online: 22 July 2023

**References**

1. WHO, UNICEF (2017) Progress on drinking water, sanitation and hygiene : 2017 update and SDG baselines. https://www.communityledtotalsanitation.org/resource/whounicef-joint-monitoring-programme-2017-report. Accessed 27 Feb 2022
2. Chilundo RJ, Neves D, Mahanjane US (2019) Photovoltaic water pumping systems for horticultural crops irrigation: advancements and opportunities towards a green energy strategy for Mozambique. Sustain Energ Technol Assess 33:61–68. https://doi.org/10.1016/j.seta.2019.03.004
3. Meunier S et al (2018) Influence of The Temporal Resolution of The Water Consumption Profile on Photovoltaic Water Pumping Systems Modelling and Sizing. 2018 7th International Conference on Renewable Energy Research and Applications (ICRERA). IEEE, Paris 2018, p 494–499. https://doi.org/10.1109/ICRERA.2018.8566828
4. Vakilifard N, Anda M, Bahri PA, Ho G, (2018) The role of water-energy nexus in optimising water supply systems review of techniques and approaches. Renew Sust Energ Rev 82:1424–1432. https://doi.org/10.1016/j.rser.2017.05.125
5. Dong W, Yang Q (2020) Data-driven solution for optimal pumping units scheduling of smart water conservancy. IEEE Internet Things J 7(3):1919–1926. https://doi.org/10.1109/jiot.2019.2963250
6. Luna T, Ribau J, Figueiredo D, Alves R (2019) Improving energy efficiency in water supply systems with pump scheduling optimization. J Clean Prod 213:342–356. https://doi.org/10.1016/j.jclepro.2018.12.190
7. Jafari-Asl J, Azizyan G, Monfared SAH, Rashki M, Andrade-Campos AG (2021) An enhanced binary dragonfly algorithm based on a v-shaped transfer function for optimization of pump scheduling program in water supply systems (case study of Iran). Eng Fail Anal 123:105323. https://doi.org/10.1016/j.engfailanal.2021.105323
8. Zhuan X, Xia X (2013) Optimal operation scheduling of a pumping station with multiple pumps. Appl Energy 104:250–257. https://doi.org/10.1016/j.apenergy.2012.10.028
9. Javan Salehi M, Shourian M (2021) Comparative application of model predictive control and particle swarm optimization in optimum operation of a large-scale water transfer system. Water Resour Manag 35(2):707–727. https://doi.org/10.1007/s11269-020-02755-6
10. Njepu A, Zhang L, Xia X (2019) Optimal pump operation for residential water supply system. Presented at International Conference on Applied Energy, Vasteras
11. Naval N, Yusta JM (2021) Optimal short-term water-energy dispatch for pumping stations with grid-connected photovoltaic self-generation. J Clean Prod 316:128386. https://doi.org/10.1016/j.jclepro.2021.128386
12. Quintiliani C, Creaco E (2019) Using additional time slots for improving pump control optimization based on trigger levels. Water Resour Manag 33(9):3175–3186. https://doi.org/10.1007/s11269-019-02297-6
13. Tadokoro H, Koibuchi H, Takahashi S, Kakudou S, Takata Y, Moriya D, Sasakawa M (2019) Water supply control system for smarter electricity power usage adopting demand-response scheme. Water Supply 20(1):140–147. https://doi.org/10.2166/ws.2019.143
14. Sichilalu S, Tazvinga H, Xia X (2016) Optimal control of a fuel cell/wind/PV/grid hybrid system with thermal heat pump load. Sol Energy 135:59–69. https://doi.org/10.1016/j.solener.2016.05.028
15. Kusakana K (2018) Optimal operation scheduling of grid-connected PV with ground pumped hydro storage system for cost reduction in small farming activities. J Energy Storage 16:133–138. https://doi.org/10.1016/j.est.2018.01.007

16. Shirinda K, Kusakana K, Koko S (2020) Techno-economic analysis of a grid-connected photovoltaic with groundwater pumped hydro storage for commercial farming activities. Int J Simul Syst Sci Technol 21:2. https://doi.org/10.5013/ijssst.a.21.02.29
17. Ngancha P, Kusakana K, Markus E (2022) Optimal pumping scheduling for municipal water storage systems. Energy Rep 8:1126–1137. https://doi.org/10.1016/j.egyr.2021.10.111
18. Shirinda K, Kusakana K, Koko SP (2020). Optimal power dispatch of a grid-connected photovoltaic with groundwater pumped-hydro storage system supplying a farmhouse. https://doi.org/10.1109/ICSGCE49177.2020.9275604
19. Kusakana K (2019) Optimal electricity cost minimization of a grid-interactive pumped hydro storage using ground water in a dynamic electricity pricing environment. Energy Rep 5:159–169. https://doi.org/10.1016/j.egyr.2019.01.004
20. Kusakana K (2018) Minimizing diesel running cost using PV with groundwater pumped hydro storage. Paper presented at IEEE Canadian Conference on Electrical & Computer Engineering (CCECE) in 2018. https://ieeexplore.ieee.org/abstract/document/8447565. Accessed 20 July 2022
21. Santos MO, Soler EM, Furlan MR, Vieira J, (2022) A mixed integer programming model and solution method for the operation of an integrated water supply system. Int Trans Oper Res 29:929–958. https://doi.org/10.1111/itor.12813
22. Shafi U, Mumtaz R, García-Nieto J, Hassan SA, Zaidi SAR, Iqbal N (2019) Precision agriculture techniques and practices: from considerations to applications. Sensors (Basel, Switzerland) 19:3796. https://doi.org/10.3390/s19173796. https://www.ncbi.nlm.nih.gov/pubmed/31480709. Accessed 15 May 2023
23. Onwude DI, Abdulstter R, Gomes C, Hashim N (2016) Mechanisation of large-scale agricultural fields in developing countries - a review. J Sci Food Agric 96:3969–3976. https://doi.org/10.1002/jsfa.7699
24. Mizik T (2022) How can precision farming work on a small scale? a systematic literature review. Precis Agric. https://doi.org/10.1007/s11119-022-09934-y
25. European Commission (2022) PVGIS Photovoltaic Geographical Information System. https://re.jrc.ec.europa.eu/pvg_tools/en/, https://joint-research-centre.ec.europa.eu/pvgis-photovoltaic-geographical-information-system_en. Accessed 20 Jan 2022
26. Palmer D, Blanchard R (2021) Evaluation of high-resolution satellite-derived solar radiation data for PV performance simulation in East Africa. Sustainability 13. https://doi.org/10.3390/su132111852
27. Sunverter 2 AC solar pump controller installation & operating manual. https://www.davisandshirtliff.com/media/com_hikashop/upload/safe/dayliff_sunverter_ii_601677142.pdf. Accessed 9 July 2022
28. Nassar YF, Salem AA (2007) The reliability of the photovoltaic utilization in southern cities of Libya. Desalination 209:86–90. https://doi.org/10.1016/j.desal.2007.04.013
29. Ndwali K, Njiri JG, Wanjiru EM (2020) Multi-objective optimal sizing of grid connected photovoltaic batteryless system minimizing the total life cycle cost and the grid energy. Renew Energy 148:1256–1265. https://doi.org/10.1016/j.renene.2019.10.065
30. Kristoffer Welsien RK Christopher Purcell, Batarda C (2018) Solar pumping: the basics. https://openknowledge.worldbank.org/entities/publication/b5dfe6fa-a842-5fcc-a28d-3c1e87d13c3a. Accessed 17 Mar 2022
31. Wanjiru EM, Sichilalu SM, Xia X (2017) Optimal control of heat pump water heater-instantaneous shower using integrated renewable-grid energy systems. Appl Energy 201:332–342. https://doi.org/10.1016/j.apenergy.2016.10.041
32. Mathaba T, Xia X, Zhang J (2014) Analysing the economic benefit of electricity price forecast in industrial load scheduling. Electr Power Syst Res 116:158–165. https://doi.org/10.1016/j.epsr.2014.05.008

## Publisher's note